



## NRC Publications Archive Archives des publications du CNRC

### **A hybrid fuzzy logic proportional-integral-derivative and conventional on-off controller for morphing wing actuation using shape memory alloy: part 1, morphing system mechanisms and controller architecture design**

Grigorie, T. L.; Botez, R. M.; Popov, A. V.; Mamou, M.; Mébarki, Y.

This publication could be one of several versions: author's original, accepted manuscript or the publisher's version. / La version de cette publication peut être l'une des suivantes : la version prépublication de l'auteur, la version acceptée du manuscrit ou la version de l'éditeur.

For the publisher's version, please access the DOI link below. / Pour consulter la version de l'éditeur, utilisez le lien DOI ci-dessous.

#### **Publisher's version / Version de l'éditeur:**

<https://doi.org/10.1017/S0001924000006977>

*The Aeronautical Journal*, 116, 1179, pp. 433-449, 2012-05

#### **NRC Publications Record / Notice d'Archives des publications de CNRC:**

<https://nrc-publications.canada.ca/eng/view/object/?id=09754f89-50a9-46b8-b57c-53c657e4118c>

<https://publications-cnrc.canada.ca/fra/voir/objet/?id=09754f89-50a9-46b8-b57c-53c657e4118c>

Access and use of this website and the material on it are subject to the Terms and Conditions set forth at

<https://nrc-publications.canada.ca/eng/copyright>

READ THESE TERMS AND CONDITIONS CAREFULLY BEFORE USING THIS WEBSITE.

L'accès à ce site Web et l'utilisation de son contenu sont assujettis aux conditions présentées dans le site

<https://publications-cnrc.canada.ca/fra/droits>

LISEZ CES CONDITIONS ATTENTIVEMENT AVANT D'UTILISER CE SITE WEB.

**Questions?** Contact the NRC Publications Archive team at

PublicationsArchive-ArchivesPublications@nrc-cnrc.gc.ca. If you wish to email the authors directly, please see the first page of the publication for their contact information.

**Vous avez des questions?** Nous pouvons vous aider. Pour communiquer directement avec un auteur, consultez la première page de la revue dans laquelle son article a été publié afin de trouver ses coordonnées. Si vous n'arrivez pas à les repérer, communiquez avec nous à PublicationsArchive-ArchivesPublications@nrc-cnrc.gc.ca.



# A Hybrid Fuzzy Logic Proportional-Integral-Derivative and Conventional On-Off Controller for Morphing Wing Actuation using Shape Memory Alloy

## Part 1: Morphing system mechanisms and controller architecture design

Teodor Lucian Grigorie, Ruxandra Mihaela Botez, Andrei Vladimir Popov  
*École de Technologie Supérieure, Montréal, Québec H3C 1K3, Canada*

Mahmoud Mamou and Youssef Mébarki  
*National Research Council, Ottawa, Ontario K1A 0R6, Canada*

### Nomenclature

$A$	=	fuzzy set in the antecedent
$A_q^i$	=	associated individual antecedent fuzzy sets of each input variable
$a_k^i$	=	parameters of the linear function
$B$	=	fuzzy set in the antecedent
$b_0^i$	=	scalar offset
$dY_1, dY_2$	=	displacements of the two control points of the flexible skin
$dY_{1opt}$	=	optimal vertical displacement of actuator 1
$dY_{2opt}$	=	optimal vertical displacement of actuator 2
$dY_{1real}$	=	real vertical displacement of actuator 1
$dY_{2real}$	=	real vertical displacement of actuator 2
$e$	=	actuation loop error
FLC	=	Fuzzy Logic Controller
FP	=	fuzzy proportional controller
$F_{aero}$	=	aerodynamic force
$F_{skin}$	=	elastic force produced by the flexible skin
$F_{spring}$	=	elastic force of the gas spring
$f$	=	a crisp function in the consequent (a polynomial function)
$i(t)$	=	command variable (electrical current in the present case)
$K_D$	=	derivative gain
$K_I$	=	integral gain
$K_O$	=	change in output gain

$K_P$	=	proportional gain
$k$	=	discrete step
$M$	=	Mach number
$mf$	=	membership function
$N$	=	number of rules
$q$	=	number of inputs
$Re$	=	Reynolds number
$T_D$	=	derivative time constant
$T_s$	=	sample period
$t$	=	time
$w^i(\mathbf{x})$	=	degree of fulfillment of the antecedent, i.e., the level of firing of the $i^{\text{th}}$ rule
$x$	=	independent variable on the universe of discourse
$x_{left}$	=	left breakpoint
$x_q$	=	individual input variables
$x_{right}$	=	right breakpoint
$\mathbf{x}$	=	input vector
$y$	=	output of the fuzzy model
$y^i$	=	first-order polynomial function in the consequent
$\Delta e$	=	actuation loop change in error
$\alpha$	=	angle of attack

## Keywords

morphing wing, actuation mechanism, smart material actuators, control design, fuzzy logic

## Abstract

The present paper describes the design of a hybrid actuation control concept, a fuzzy logic Proportional-Integral-Derivative plus a conventional On-Off controller, for a new morphing mechanism using smart materials as actuators, which were made from Shape Memory Alloys (SMA). The research work described here was developed for the open loop phase of a morphing wing system, whose primary goal was to reduce the wing drag by delaying the transition (from laminar to fully turbulent

flows) position toward the wing trailing edge. The designed controller drives the actuation system equipped with SMA actuators to modify the flexible upper wing skin surface. The designed controller was also included, as an internal loop, in the closed loop architecture of the morphing wing system, based on the pressure information received from the flexible skin mounted pressure sensors and on the estimation of the transition location.

The controller's purposes were established following a comprehensive presentation of the morphing wing system architecture and requirements. The strong nonlinearities of the SMA actuators' characteristics and the system requirements led to the choice of a hybrid controller architecture as a combination of a bi-positional on-off controller and a Fuzzy Logic Controller (FLC). In the chosen architecture, the controller would behave as a switch between the SMA cooling and heating phases, situations where the output current is 0 A or is controlled by the FLC.

In the design phase, a Proportional-Integral-Derivative scheme was chosen for the FLC. The input-output mapping of the fuzzy model was designed, taking account of the system's error and its change in error, and a final architecture for the hybrid controller was obtained. The shapes chosen for the inputs' membership functions were *s*-function,  $\pi$ -function, and *z*-function, and product fuzzy inference and the center average defuzzifier were applied (Sugeno).

## **1. Introduction**

In the aerospace vehicle field, wing morphing refers to the ability of an aircraft wing to change shape during flight, thereby providing aerodynamic performance advantages. The wing morphing approach is referred to as the variform wing concept. In this way, a morphing wing can be considered as a wing that has the ability to either alter its shape in a continuous change along the chord or spar, or to change its shape in a drastic manner [1]-[3]. The highest present demand on fuel consumption has emphasized the importance of improving aerodynamic efficiency through modification of the wing geometry that can move the laminar-to-turbulent transition point close to the wing trailing edge, thus reducing the drag [4]. Many theoretical and experimental studies on morphing wings have been developed. These studies began with work on independent airfoils and have been extended to different airplane configurations, especially UAV's. A broad range of aerodynamic optimization strategies have already been adopted into airplane design.

Recently, morphing wing system studies have branched out into new research directions. Developments in the smart materials field have spurred research on morphing wings, considering their possible use in the design of intelligent wings. One of the biggest morphing projects is the NASA Aircraft Morphing Program, which focuses on developing smart devices to be used in airframe applications to achieve significant improvements in aircraft efficiency and affordability. As smart materials, shape-memory alloys were used to create shape changes in a wing [5]. Many academia, such as Virginia Polytechnic, State

University, University of Florida, University of Maryland, Texas A&M University, Delft University and Bristol University, are also engaged in research on morphing wings and have developed various experimental models. In order to achieve the optimal outcomes imposed by the aerodynamic studies, the actuation line of the morphing structure must be precisely controlled. Several control strategies have been adopted as complex functions of the morphing structure and of the actuator types in various morphing applications [6]-[10].

The global technological evolution has led to the increasing complexity of applications developed in industry and in scientific research fields. Therefore, many researchers have focused their efforts on providing simple control algorithms to cope with the increasing complexity of the controlled systems [11]. The main challenge of a control designer is to find a formal way to convert the knowledge and experience of a system operator into a well-designed control algorithm [12]. From another perspective, the control design method should allow full flexibility in the adjustment of the control surface; taking into account that the systems involved in practice are, generally, complex, strongly nonlinear and often with poorly defined dynamics [11]. If a conventional control methodology, based on linear system theory, is used, a linearized model of the nonlinear system should be developed in advance. Because the validity of a linearized model is limited to a range around the operating point, any guarantee of good performance cannot be provided by a controller obtained in this manner. Therefore, to achieve satisfactory control of a complex nonlinear system, a nonlinear controller must be developed [11]-[14]. From another viewpoint, if it would be difficult to describe the controlled system precisely by conventional mathematical relations, then the design of a controller based on classical analytical methods would be totally impractical [12], [14]. With such systems, there is a motivated interest in using a control designed by a skilled operator, based on years of experience and knowledge about the static and dynamic characteristics of the system; the controller is known as a Fuzzy Logic Controller (FLC) [14]. FLCs are based on fuzzy logic theory, developed by L. Zadeh [15]. By using multivalent fuzzy logic, linguistic expressions in antecedent and consequent parts of IF-THEN rules describing the operator's actions can be efficiently converted into a fully-structured control algorithm suitable for microcomputer implementation or implementation with specially designed fuzzy processors [12]. In contrast with traditional linear and nonlinear control theory, an FLC is not based on a mathematical model, and it provides a certain level of artificial intelligence to the conventional PID controllers [11].

Some of the most important applications of the fuzzy logic theories in the aerospace field include: the performance of both stability augmentation and automatic flight control functions for the longitudinal and lateral-directional motions for an X-29 aircraft [16], the development of a pitch attitude hold system for a typical fighter jet under a variety of performance conditions that include approach, subsonic cruise and supersonic cruise [17], the design of a flight control system and navigation tasks for autonomous unmanned aerial vehicles [18], the development of an intelligent Anti-lock Braking System (ABS) control for an aircraft [19], [20], the development of an augmented flight control for an F16 aircraft [21], and the representation,

manipulation and utilization of aerodynamic characteristics in order to model an aircraft with and without winglets [22]. Another application was implemented in a new method for aerodynamic forces conversion from a frequency to a Laplace domain, which was validated on the F/A-18 aircraft for aeroservoelasticity studies [23]. The F/A-18 aircraft non-linear model was identified from flight flutter tests by use of fuzzy logic [24] and a combination of fuzzy logic and neural network methods [25].

This paper presents approaches for the design and validation of a hybrid fuzzy logic proportional-integral-derivative plus conventional on-off controller used in the actuation of a morphing wing. This research work was a part of a large scale morphing wing project, developed with the goal of reducing operating costs for the new generation of aircraft through fuel consumption economy in flight, and also to improve aircraft performance, expanding flight envelopes, replacing conventional control surfaces, reducing drag to improve range and reduce vibrations and flutter. The actuation control concept of the morphing wing uses smart materials such as Shape Memory Alloy (SMA) as actuators. The smart actuators deform dynamically the upper wing surface flexible skin with the aim to delay laminar-to-turbulent flow transition point towards the wing trailing edge [4].

## **2. Morphing wing project**

The morphing wing research work is a multi-partner project which was mainly funded by the Consortium for Research and Innovation in Aerospace in Quebec (CRIAQ) in collaboration with universities and industries. The project is entitled “*Laminar Flow Improvement on an Aeroelastic Research Wing*”, with the main objective to reduce wing form drag by controlling the boundary layer flow behavior on the wing surface. In other words, the wing skin shape is adapting its self automatically to keep the transition point position always close to the wing trailing edge. This project was initiated and funded by aerospace companies Bombardier Aerospace and Thales Avionics, as well as by CRIAQ and the Natural Sciences and Engineering Research Council of Canada (NSERC), and developed by the Ecole de Technologie Supérieure in Montréal (ETS) and the Ecole Polytechnique in Montréal (EP) in collaboration with the Institute for Aerospace Research at the National Research Council Canada (IAR-NRC).

The objectives of the project achieved by ETS *Research Laboratory in Active Controls, Avionics and Aeroservoelasticity* (LARCASE) were to develop a system for the active control of a morphing wing during flight to maintain large laminar flow run over the upper surface of the wing, and to detect the surface airflow behaviour using pressure sensors installed on the wing skin surface. To this end, numerical simulations and experimental multidisciplinary studies via bench tests and wind tunnel measurements were performed for a morphing wing equipped with a flexible skin, SMA smart material actuators and pressure

sensors. Over the course of this research project, investigations were realized on: optical and Kulite sensors' selection and testing for laminar to turbulent flow transition validation (by use of Xfoil code and Matlab); smart material actuators' controller methods; aero-elasticity wing studies using MSC/Nastran; open loop and closed loop transition delay controller design; integration and validation on the wing equipped with SMA smart material actuators and pressure sensors (simulation versus test results) [4], [26]-[29]. A thorough validation exercise was performed by comparing the predicting results to the experimental bench and wind tunnel data.

The work described here was developed in the open loop phase of the morphing wing system. The wing model considered was a rectangular plan form wing (0.54 m x 0.9 m), based on the WTEA-TE1 reference airfoil (Fig. 1). The lower part of the mechanical model is an aluminium block designed to allow space for the wiring, while the upper part has an aluminium structure equipped with a flexible skin made of composite materials (layers of carbon and Kevlar fibers in a resin matrix) and with the actuation system (Shape Memory Actuators (Ni-Ti)). A number of 35 flow conditions were established as a combination of five Mach numbers (0.2, 0.225, 0.25, 0.275, 0.3) and seven incidence angles ( $-1^\circ$ ,  $-0.5^\circ$ ,  $0^\circ$ ,  $0.5^\circ$ ,  $1^\circ$ ,  $1.5^\circ$ ,  $2^\circ$ ) to test the morphed structure. Thus, starting from the reference airfoil, 35 optimized airfoils were designed based on the flow conditions [30].

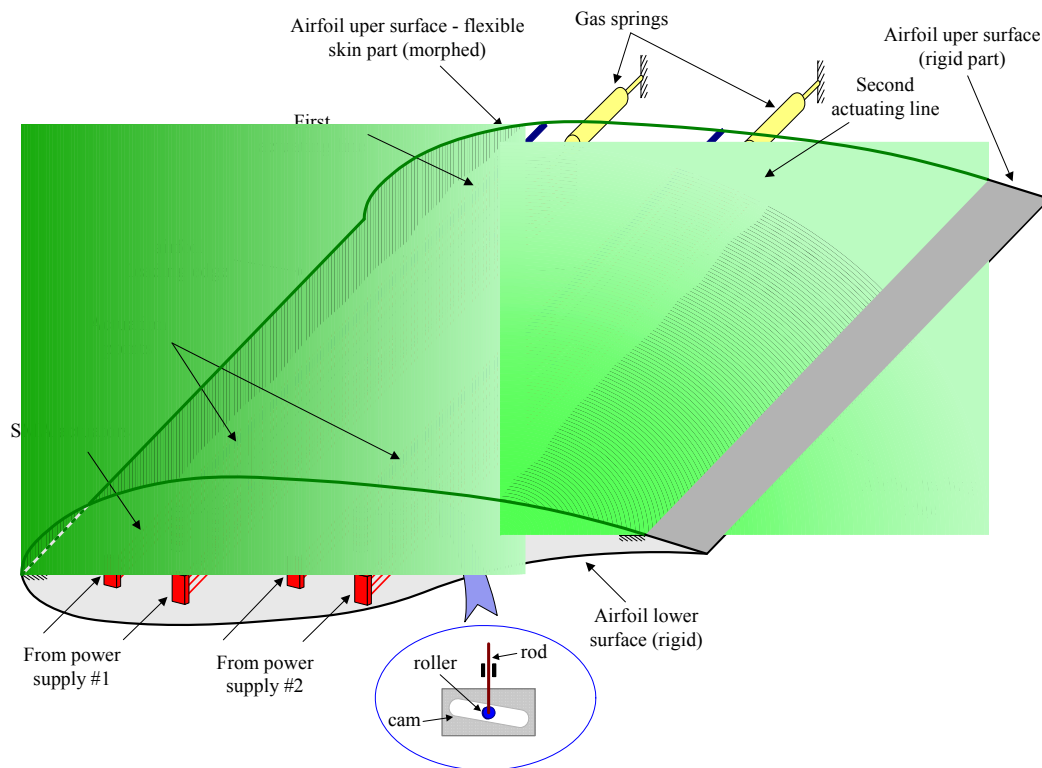


Fig. 1 Morphing wing model.

From the initial studies related to the optimal configuration of the flexible structure, two actuation lines, positioned at 25.3% and 47.6% of the chord, from the airfoil leading edge, were chosen to morph the flexible skin [31]-[34]. In order to achieve an

optimized airfoil shape for theoretical flow conditions, the flexible skin was required to morph its shape through two actuation points. Two shape memory alloy actuators, of non-linear behavior, drove the displacement ( $dY_1, dY_2$ ) of the two control points of the flexible skin towards the optimized airfoil shape. Each of the shape memory actuators was activated by a power supply unit and were controlled so as to morph the flexible skin until the obtained (real) displacements ( $dY_{1real}, dY_{2real}$ ) become equal with the desired (optimal) displacements ( $dY_{1opt}, dY_{2opt}$ ), calculated as differences between the optimized airfoils and the reference airfoil at the control points level. The real deflections of the morphed structure were monitored using two position transducers.

### 3. Hybrid controller purposes

A block diagram of the open loop controlled morphing wing system, based on the previous considerations, is shown in Fig. 2.

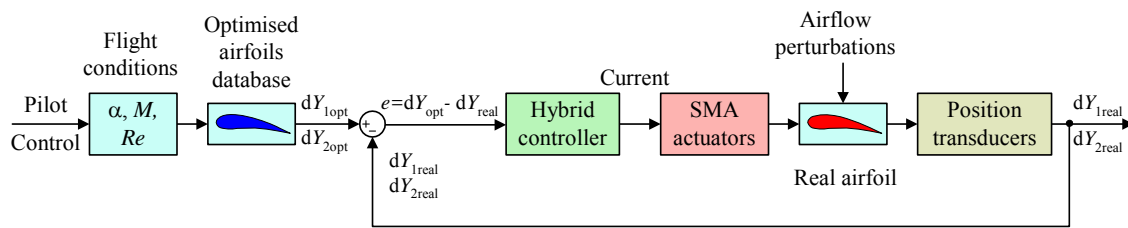


Fig. 2 Block diagram of the open loop controlled morphing wing system.

SMA actuator control can be achieved using any method of position control; however, the specific properties of the SMA actuators, such as hysteresis, the first cycle effect and the impact of long-term changes, must be considered. At the same time, the realistic requirements of our system displacements must also be considered.

SMA wires can process the deflections obtained using the applied forces and provide a variety of shapes and sizes that are extremely useful to achieve actuation system goals. For example, SMA wires can provide high forces corresponding to small strains to achieve the right balance between the forces and the deformations, as required by the actuation system. To ensure a stable system, a compromise or balance must be established and maintained. The structural components of the actuation system should be designed to respect the actuators' capabilities to reliably obtain the required deflections and forces.

Despite their simplistic design and mechanical performance, SMAs have their disadvantages. They require a high current to heat rapidly rise their temperature to the material lattice transformation and maintain the current to withstand the displacement. This is translated directly to a significant amount of energy waist. Their volumes are maintained during the entire transformation process; their lengths decrease while their diameters increase. There are also other problems with their attachment to other structures. The wires cannot be directly soldered or epoxied to a surface, as after several cycles of



operation, the attachment would be broken. Another issue is that the wire's reliability decreases when over-heated or over-strained. Over-heating or over-straining reduced considerably the number of operation cycles from thousands to only few hundreds. Overall, the SMA actuator's disadvantages were deemed to be very small and manageable compared to the problems associated with the other types of smart actuators.

In the present investigation, each of the actuation lines uses three SMA wires as actuators, and contains a cam, which moves in translation relative to the structure (see Fig. 1). The cam causes the rod motion related to the roller and the skin. A compression gas spring is also used as recall. When the SMA is heated the actuator contracts and the cam moves to the right, resulting in the rise of the roller and the displacement of the skin upwards. Cooling of the SMA, results in a cam motion to the left, and thus a movement of the skin downwards. The horizontal displacement of each actuator is converted into a vertical displacement at a rate of 3:1, which gives the conversion of the horizontal stroke of  $x$  mm into a vertical stroke  $y = x/3$ . From the optimized airfoils, an approximately 8 mm maximum vertical displacement is obtained for the rods, which requires a maximum horizontal displacement of 24 mm for the actuators.

In the literature, the modeling and control of smart material actuators are relatively recent research fields. Technical literature is available in three independent domains: modeling, control, and smart materials. A smart actuator is formulated for a large range of smart materials and devices, and can be found in a variety of different configurations. It is common knowledge that all physical systems, including smart actuators, contain nonlinearities. As a consequence, smart material actuators can be linearly modeled and may contain errors, while they can also be non-linearly modeled.

The non-linear model used to design and numerically simulate the controller is based on finite element method; the model was built in the Shape Memory Alloys and Intelligent Systems Laboratory (LAMSI) at ETS, using Lickhatchev's theoretical model [35]. The inputs of the SMA model are the alloy initial temperature, the electrical current and the applied force. The outputs are the actuator displacement and the alloy temperature during its functioning. To use the SMA shape-changing characteristics, an initialization by an external force is required, which obliges it to pass first through the transformation phase and then to return it to the initial phase after the cooling phase. The control could not be realized, due to the intrinsic behavior of the SMA [29], [35].

The simulation model shown in Fig. 3 was obtained by implementing the SMA actuator model using a Matlab S-function. To control the SMA actuators, they need to be supplied with an adequate electrical current. The length of the SMA wires is a complex function of the SMA load forces and temperatures, the latter factor being influenced by the supplying current over time and by the interaction of the wires with the environment in the cooling phase (when the electrical supply is switched off) [26], [27]. The "Mechanical system" block considers the forces influencing the SMA load force: the aerodynamic force  $F_{aero}$ , the skin force  $F_{skin}$ , and the gas spring force  $F_{spring}$ .

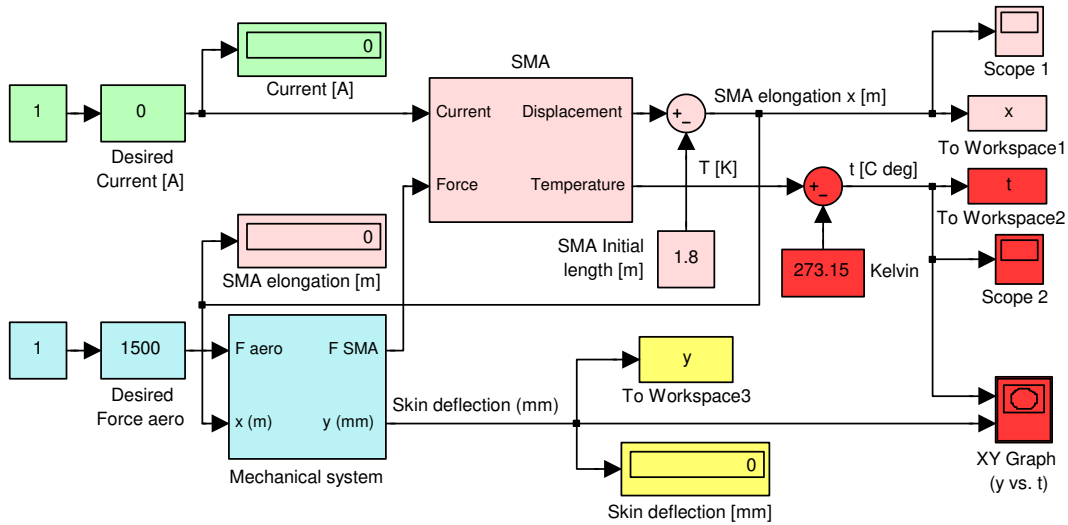


Fig. 3 SMA actuators' Matlab/Simulink simulation model.

The envelope of the SMA actuator 1 or 2, obtained through numerical simulations for different aerodynamic load cases, is shown in Fig. 4, where the SMA initial wire length is equal to 1.8 m. As can be observed in Fig. 4, to obtain a skin maximum vertical displacement (8 mm) in the absence of aerodynamic forces, a high temperature, of approximately 162°C, is needed to counteract the spring force. Since the ability of the SMA wires to contract is dependent upon Joule heating to produce the required transformation temperature, the need for a higher temperature is reflected by a need for higher electrical current. Also, the envelope in Fig. 4 confirms the strong nonlinear character of the SMA actuator as a function of the load force and temperature.

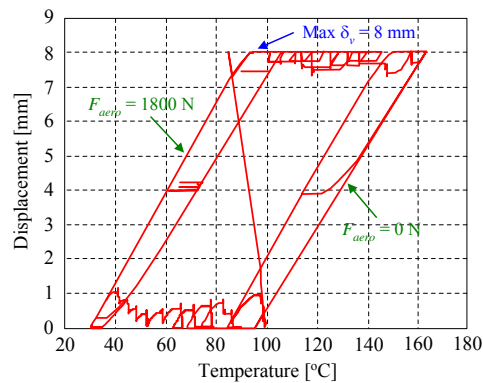


Fig. 4 SMA actuator simulated envelope.

As shown in Fig. 2, the hybrid controller's purpose is to control the SMA actuators by means of the electrical current supply, in order to cancel the deviation  $e$  between the required values for vertical displacements (corresponding to the optimized airfoils) and the real values, obtained from position transducers. As mentioned previously, the design of such a controller is difficult due to the strong nonlinearities of the SMA actuators' characteristics; these nonlinearities are significantly influenced by the stressing forces. Given these conditions, and considering our research team's experience in fuzzy logic control systems

design as well as in SMA modeling, it was decided that one variant of control would be developed with fuzzy logic. On the other hand, because it is normal that in the SMA cooling phase the actuators would not be powered, we adopt a combination of a bi-positional (particularly an on-off one) and a fuzzy logic controller (FLC) for our morphing wing application. This cooling phase may occur not only when controlling a long-term phase, when a switch between two values of the actuator displacements is commended, but also in a short-lived phase, which happens when the real value of the deformation exceeds its desired value and the actuator wires need to be cooled. As a consequence, the hybrid controller should behave as a switch between the SMA cooling and heating phases, in which the output current is 0 A, or is controlled by the FLC.

## 4. Hybrid controller design

### 4.1. FLC structure

Fuzzy logic is an innovative technology that provides tool to interpret the human experience into reality, which enhances conventional system design with engineering expertise. The use of fuzzy logic can help to circumvent the need for rigorous mathematical modeling, which is a very difficult if not an impossible task. Fuzzy logic controllers are rule-based controllers. The basic configuration of a fuzzy logic model can be represented in four parts, as shown in Fig. 5: the fuzzifier, the inference engine, the defuzzifier, and a knowledge base. The fuzzifier reads, measures, scales the control variable, and transforms the measured numerical values to the corresponding linguistic variables with appropriate membership values. The knowledge base includes the definitions of the fuzzy membership functions defined for each control variable and the required (IF-THEN) rules that specify the control goals using linguistic variables. The inference engine calls the fuzzy rule base to derive the linguistic values for the output linguistic variables. The defuzzifier converts the inferred decision from the linguistic variables back to the numerical values. The development of a control system based on fuzzy logic thus involves the following steps: fuzzification strategy, data base building, rule base elaboration, inference machine elaboration and defuzzification strategy [36], [37].

The simplest fuzzy logic controller is the proportional controller (FP), appropriate for a state or an output feedback in a state space controller. Its input is the error and the output is the control signal. From another perspective, derivative action helps to predict the error, and the proportional-derivative (PD) controller makes further use of the derivative action to improve closed-loop stability [38]. The equation of a PD controller can be expressed as follows:

$$i(t) = K_p \cdot e(t) + K_d \cdot \frac{de(t)}{dt} = K_p \cdot \left[ e(t) + T_d \cdot \frac{de(t)}{dt} \right], \quad (1)$$

where  $i(t)$  is the command variable (electrical current in the present case), and is time dependent;  $e$  is the operating error (see

Fig. 2),  $K_p$  is the proportional gain and  $K_D$  is the derivative gain. The control signal is thus proportional to an estimate of the error  $T_D$  seconds ahead, where the estimate is obtained by linear extrapolation. If the  $T_D$  time constant is zero, the controller becomes a purely proportional one. The gradual increase of the  $T_D$  value will produce damped oscillations of the system; over a threshold value the system becomes overdamped [38].

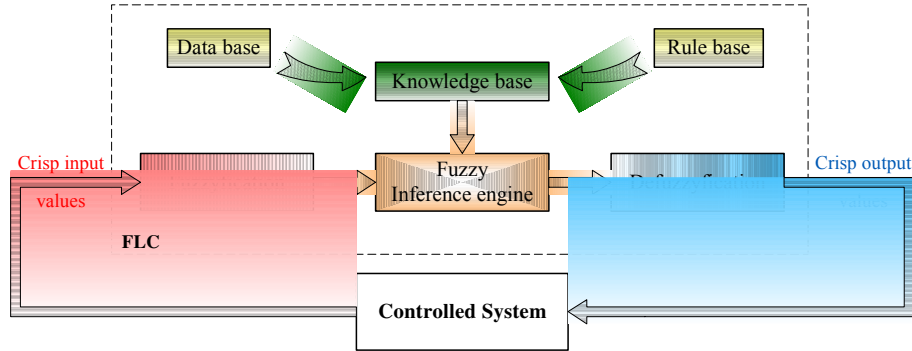


Fig. 5 Block diagram of the FLC.

In discrete form, the equation (1) becomes [39]:

$$i(k) = K_p \cdot e(k) + K_D \cdot \Delta e(k), \quad (2)$$

or

$$i(k) = K_p \cdot e(k) + K_D \cdot \frac{[e(k) - e(k-1)]}{T_s}, \quad (3)$$

where  $k$  is the discrete step,  $T_s$  is the sample period and  $\Delta e(k)$  is the change in error. Therefore, the inputs to the fuzzy proportional-derivative (FPD) controller are the error and its derivative (called change in error in fuzzy control language).

Additionally, if there is a sustained steady state error, integral action is absolutely necessary [38]. Considering the control law of a proportional-integral (PI) controller is easier to find from its discrete form that for a fuzzy PI controller obtaining are also used the error and change in error as inputs to the rule base [39]. Literature review has indicated that it is rather difficult to write rules for the integral action, because the integrator windup problem appears due to the physical limitations of the actuator; after the saturation, the control action stays constant, but the error continues to be integrated and the integrator winds up [38].

Two methods to obtain a fuzzy controller with an integral component and avoid the integrator windup problem are proposed in [38]: a fuzzy incremental controller architecture (Fig. 6. a) and a parallel integral action with a fuzzy PD architecture (Fig. 6.b).

In [39], two equivalent architectures for a fuzzy PID controller are given: a) fuzzy PI + fuzzy PD in feedback mode and b) fuzzy PI + fuzzy PD in cascade configuration.

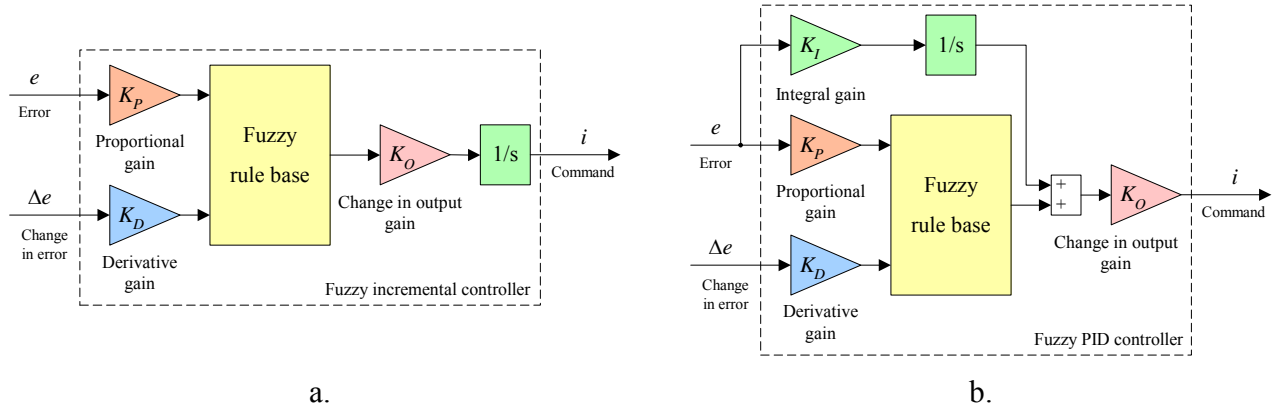


Fig. 6 Fuzzy controller architectures.

The incremental controller (see Fig. 6a) has a disadvantage in that it does not include the derivative component well [38]. To take advantage of all the benefits of a PID controller, the structure shown in Fig. 6.b for our FLC is chosen.

#### 4.2. Input-output mapping

As mentioned above, the output error ( $e$ ) and the change in error ( $\Delta e$ ) are used as controller inputs, and the electrical current  $i$  is used as the command variable (controller output). Each of the FLC input or output signals have the real line as the universe of discourse. In practice, the universe of discourse is restricted to a comparatively small interval; many authors and several commercial controllers use standard universes such as  $[-1, 1]$ , or  $[-100, 100]$  corresponding to percentages of full scale. The universe of discourse of each fuzzy variable can be quantized into a number of overlapping fuzzy sets (linguistic variables). Each element in the universe of discourse is a member of a fuzzy set to some degree; the degree of membership for all its members describes a fuzzy set. The membership function ( $mf$ ) ties a number to each element of the universe. Before designing the membership functions, it is absolutely necessary to consider the universes for the inputs and outputs [36]-[38]. For our system, the  $[-1, 1]$  interval was chosen as the universe for all of the input and output signals. Also, following numerical simulations, we chose three membership functions for each of the two inputs, and five membership functions for the output. The shapes chosen for the input membership functions were the  $s$ -function,  $z$ -function, and  $\pi$ -function. Generally, an  $s$ -function shaped membership function can be implemented using a cosine function:

$$s(x_{left}, x_{right}, x) = \begin{cases} 0, & \text{if } x < x_{left} \\ \frac{1}{2} \left[ 1 + \cos \left( \frac{x - x_{right}}{x_{right} - x_{left}} \pi \right) \right], & \text{if } x_{left} \leq x \leq x_{right} \\ 1, & \text{if } x > x_{right} \end{cases} \quad (4)$$

a  $z$ -function shaped membership function is a reflection of a shaped  $s$ -function:

$$z(x_{left}, x_{right}, x) = \begin{cases} 1, & \text{if } x < x_{left} \\ \frac{1}{2} \left[ 1 + \cos \left( \frac{x - x_{left}}{x_{right} - x_{left}} \pi \right) \right], & \text{if } x_{left} \leq x \leq x_{right} \\ 0, & \text{if } x > x_{right} \end{cases} \quad (5)$$

and a  $\pi$ -function shaped membership function is a combination of both functions:

$$\pi(x_{left}, x_{m1}, x_{m2}, x_{right}, x) = \min[s(x_{left}, x_{m1}, x), z(x_{m2}, x_{right}, x)], \quad (6)$$

with the peak flat over the  $[x_{m1}, x_{m2}]$  middle interval.  $x$  is the independent variable on the universe,  $x_{left}$  is the left breakpoint, and  $x_{right}$  is the right breakpoint [38].

To define the rules, a Sugeno fuzzy model proposed by Takagi, Sugeno and Kang [40] was selected. A Takagi, Sugeno and Kang fuzzy rule for a two input-single output system can be written in the following form:

$$\text{“if } (x_1 \text{ is } A) \text{ and } (x_2 \text{ is } B) \text{ then } y = f(x_1, x_2)\text{”}, \quad (7)$$

where  $A$  and  $B$  are fuzzy sets in the antecedent,  $y = f(x_1, x_2)$  is a crisp function in the consequent, and  $f(x_1, x_2)$  is a polynomial function. If  $f$  is a first-order polynomial, then the resulting fuzzy inference is called a first-order Sugeno fuzzy model, while if  $f$  is a constant then it is a zero-order Sugeno fuzzy model. For a two input-single output system, a first-order Sugeno fuzzy model with  $N$  rules is given by ([40]):

$$\begin{aligned} \text{Rule 1: If } x_1 \text{ is } A_1^1 \text{ and } x_2 \text{ is } A_2^1, \text{ then } y^1(x_1, x_2) &= b_0^1 + a_1^1 x_1 + a_2^1 x_2, \\ &\vdots \\ \text{Rule } i: \text{ If } x_1 \text{ is } A_1^i \text{ and } x_2 \text{ is } A_2^i, \text{ then } y^i(x_1, x_2) &= b_0^i + a_1^i x_1 + a_2^i x_2, \\ &\vdots \\ \text{Rule } N: \text{ If } x_1 \text{ is } A_1^N \text{ and } x_2 \text{ is } A_2^N, \text{ then } y^N(x_1, x_2) &= b_0^N + a_1^N x_1 + a_2^N x_2, \end{aligned} \quad (8)$$

where  $x_q$  ( $q = \overline{1,2}$ ) are the individual input variables,  $y^i$  ( $i = \overline{1,N}$ ) is the first-order polynomial function in the consequent, and  $A_q^i$  ( $i = \overline{1,N}$ ) are the associated individual antecedent fuzzy sets of each input variable. The coefficients  $a_k^i$  ( $k = \overline{1,2}, i = \overline{1,N}$ ) are parameters of the linear function, and  $b_0^i$  ( $i = \overline{1,N}$ ) denotes a scalar offset.

For any input vector,  $\mathbf{x} = [x_1, x_2]^T$ , if the singleton fuzzifier, the product fuzzy inference and the center average defuzzifier are applied (Sugeno type), then the output of the fuzzy model  $y$  is inferred as follows (weighted average) and shown in Fig 7:

$$y = \left( \sum_{i=1}^N w^i(\mathbf{x}) y^i \right) / \left( \sum_{i=1}^N w^i(\mathbf{x}) \right). \quad (9)$$

$$w^i(\mathbf{x}) = A_1^i(x_1) \times A_2^i(x_2), \quad (10)$$

which represents the degree of fulfillment of the antecedent, i.e., the level of firing of the  $i^{\text{th}}$  rule.

In the  $[-1, 1]$  universe interval, a three-range partition: negative (N), zero (Z) and positive (P), was chosen for the inputs  $e$  and  $\Delta e$ , and a five-range partition: negative-big (NB), negative-small (NS), zero (Z), positive-small (PS) and positive-big (PB) was used for the output. According to the values in Table 1, the membership functions for both inputs are in the form depicted in Fig. 8, and are given by eqs. (4), (5) or (6) as:

$$A_1^1(x) = A_2^1(x) = z(-1, 0, x) = \begin{cases} 1, & \text{if } x < -1 \\ \frac{1}{2}[1 + \cos(x+1)\pi], & \text{if } -1 \leq x \leq 0, \\ 0, & \text{if } x > 0 \end{cases} \quad (11)$$

$$A_1^2(x) = A_2^2(x) = \min[s(-1, 0, x), z(0, 1, x)] = \begin{cases} 0, & \text{if } x < -1 \\ \frac{1}{2}[1 + \cos(\pi x)], & \text{if } -1 \leq x \leq 1, \\ 0, & \text{if } x > 1 \end{cases} \quad (12)$$

$$A_1^3(x) = A_2^3(x) = s(0, 1, x) = \begin{cases} 0, & \text{if } x < 0 \\ \frac{1}{2}[1 + \cos(x-1)\pi], & \text{if } 0 \leq x \leq 1, \\ 1, & \text{if } x > 1 \end{cases} \quad (13)$$

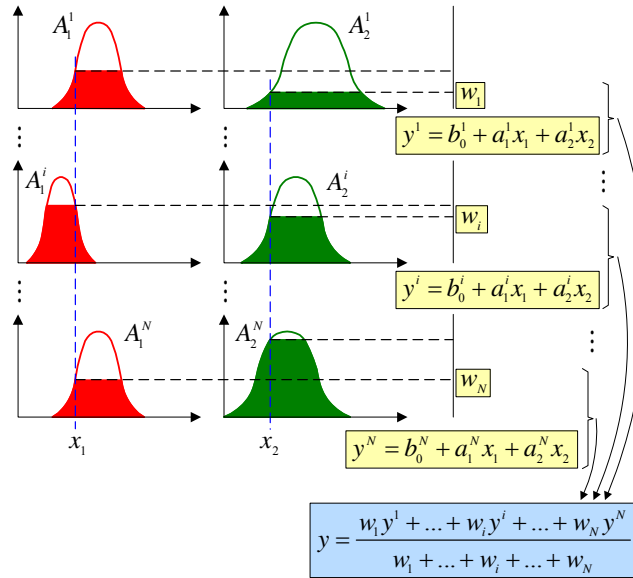


Fig. 7 Output of the fuzzy model.

**Table 1** Parameters of the inputs' membership functions

$mf$ type	$mf$ parameters	$mf$ parameters			
		$x_{left}$	$x_{m1}$	$x_{m2}$	$x_{right}$
$mf1$ ( $A_1^1$ and $A_2^1$ )	$z$ -function	-1	-	-	0
$mf2$ ( $A_1^2$ and $A_2^2$ )	$\pi$ -function	-1	0	0	1
$mf3$ ( $A_1^3$ and $A_2^3$ )	$s$ -function	0	-	-	1

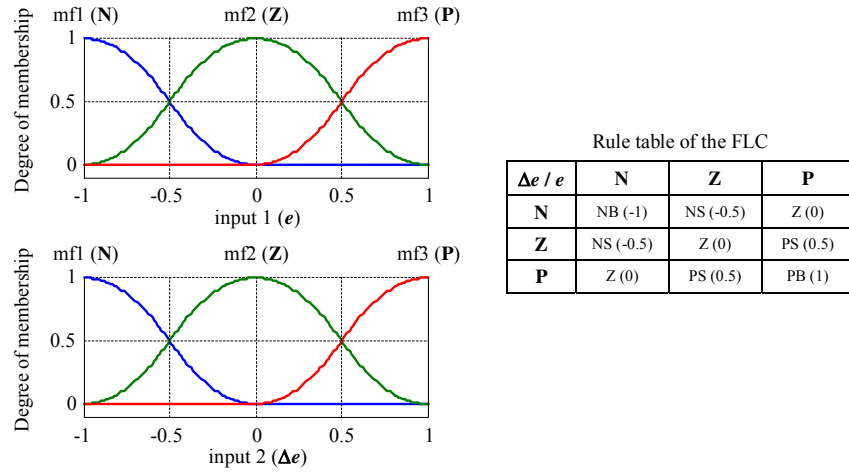


Fig. 8 Membership functions and rule-based inference for the fuzzy logic controller.

For the output membership functions, constant values were chosen (NB=-1, NS=-0.5, Z=0, PS=0.5, PB=1), so the values of the  $a_k^i$  ( $k = \overline{1,2}, i = \overline{1,N}$ ) parameters in Eq. (8) are zero. Starting from the inputs' and output's membership functions, a set of 9 inference rules were obtained ( $N=9$ ):

- Rule 1: If  $e$  is  $A_1^1$  and  $\Delta e$  is  $A_2^1$ , then  $y^1(e, \Delta e) = -1$ ,
- Rule 2: If  $e$  is  $A_1^1$  and  $\Delta e$  is  $A_2^2$ , then  $y^2(e, \Delta e) = -0.5$ ,
- Rule 3: If  $e$  is  $A_1^1$  and  $\Delta e$  is  $A_2^3$ , then  $y^3(e, \Delta e) = 0$ ,
- Rule 4: If  $e$  is  $A_1^2$  and  $\Delta e$  is  $A_2^1$ , then  $y^4(e, \Delta e) = -0.5$ ,
- Rule 5: If  $e$  is  $A_1^2$  and  $\Delta e$  is  $A_2^2$ , then  $y^5(e, \Delta e) = 0$ ,
- Rule 6: If  $e$  is  $A_1^2$  and  $\Delta e$  is  $A_2^3$ , then  $y^6(e, \Delta e) = 0.5$ ,
- Rule 7: If  $e$  is  $A_1^3$  and  $\Delta e$  is  $A_2^1$ , then  $y^7(e, \Delta e) = 0$ ,
- Rule 8: If  $e$  is  $A_1^3$  and  $\Delta e$  is  $A_2^2$ , then  $y^8(e, \Delta e) = 0.5$ ,
- Rule 9: If  $e$  is  $A_1^3$  and  $\Delta e$  is  $A_2^3$ , then  $y^9(e, \Delta e) = 1$ .

The rule-based inference chosen for each consequent is also presented in Fig. 8. With the previous considerations, the fuzzy control surface results in the form presented in Fig. 9.

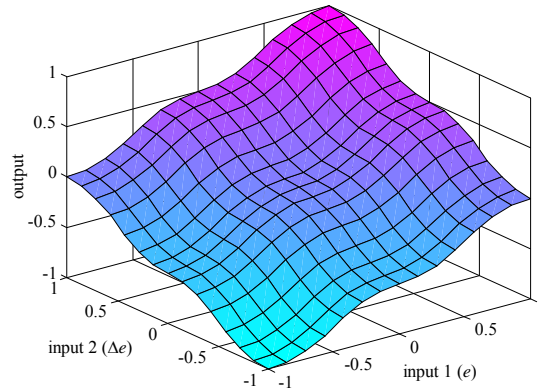


Fig. 9 The fuzzy control surface.



### 4.3. Hybrid controller resulted architecture

Starting from the observation that in the SMA cooling phase the actuators are not powered, we have chosen a combination of a bi-positional (particularly an on-off) and a fuzzy logic controller (FLC) for our morphing application. As we have stated earlier, the cooling phase may occur not only when controlling a long-term phase, when a switch between two values of the actuator displacements is ordered, but also in a short-lived phase, which occurs when the real value of the deformation exceeds its desired value. As a consequence of this need and of the previous FLC description, the resulting architecture for the hybrid controller is shown in Fig. 10.

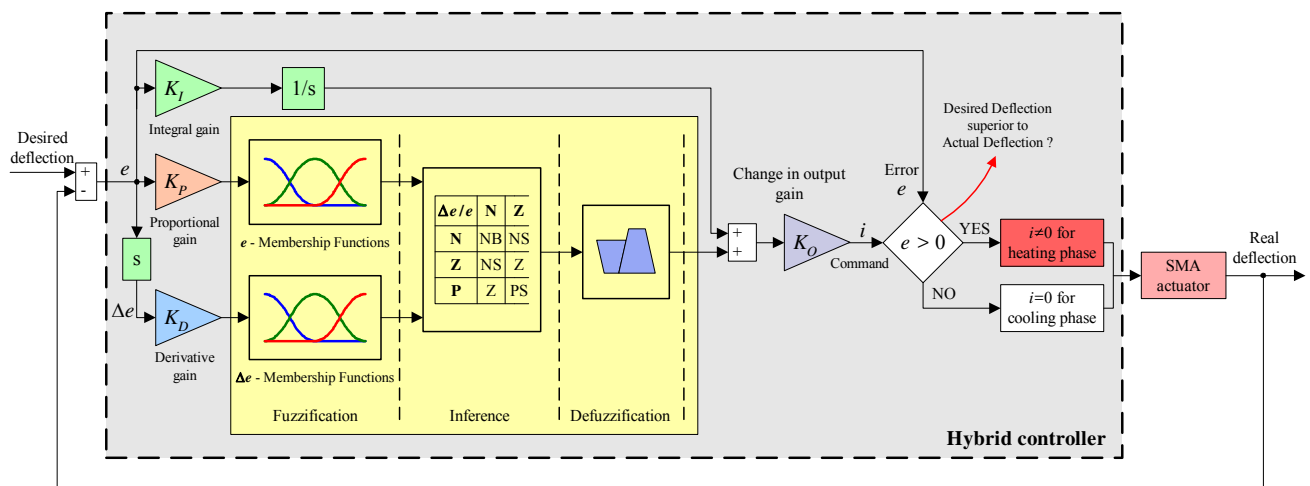


Fig. 10 Hybrid controller architecture.

### 5. Conclusions

The approaches for the design of a hybrid fuzzy logic proportional-integral-derivative plus a conventional on-off controller used in the actuation of a morphing wing were presented. The actuation control concept of the morphing wing uses smart materials such as Shape Memory Alloy (SMA) as actuators. These smart actuators modify the flexible skin upper wing surface, so that the laminar-to-turbulent transition point moves close to the wing airfoil trailing edge. The long-term goals of this research project are the reduction of operating costs for new generation aircraft through flight fuel economy, and also the improvement in aircraft performance, the expansion of aircraft flight envelopes, the replacement of conventional control surfaces, and drag reduction to improve flight range and reduce vibrations and flutter.

The envelope of the SMA actuator confirms that the length of the SMA wires is a complex function of the SMA load force and temperature, the latter influenced by the supplying current over time and by the interaction of the wires with the environment

in their cooling phase (when the electrical supply is removed). Because the ability of the SMA wires to contract is dependent on Joule heating to produce the required transformation temperature, the need for a higher temperature is reflected by a need for a higher electrical current.

To achieve the aerodynamic goal for the morphing wing (moving the laminar-to-turbulent transition point close to the wing airfoil trailing edge), a first phase of studies involved the determination of optimized airfoils available for 35 different flow conditions (combinations of five Mach numbers and seven angles of attack). The hybrid controller's purpose was the control of the SMA actuators by means of the electrical current supply, with the aim of canceling the deviations between the required values for vertical displacements (corresponding to the optimized airfoils) and the real experimental values, obtained from position transducers. Because of the strong nonlinearities of the SMA actuators' characteristics (nonlinearities that are significantly influenced by the forces employed to tense them), a fuzzy logic control variant was developed. In addition, because it is normal that the actuators are not powered in the SMA cooling phase, a combination of a bi-positional (particularly an on-off) and a fuzzy logic controller was chosen. The hybrid controller behaved as a switch between the SMA cooling and heating phases, in situations where the output current was 0 A, or it was controlled by the fuzzy logic controller. The fuzzy logic controller scheme chosen was a Proportional-Integral-Derivative. The shapes chosen for the input membership functions were the  $s$ -function,  $\pi$ -function, and  $z$ -function, and product fuzzy inference and the Sugeno center-average defuzzifier were applied.

After this preliminary design step, a complete validation cycle of the hybrid controller was realized (numerical simulations, experimental bench test in laboratory conditions without aerodynamic force loads, and a final wind tunnel test) and will be presented in the second part of this paper.

## **Acknowledgements**

The authors would like to thank the Consortium for Research and Innovation in Aerospace in Quebec (CRIAQ), Thales Canada and Bombardier Aerospace for their financial and technical support. The authors also wish to express their appreciation to Mr. George Henri Simon for initiating the CRIAQ 7.1 project and to Mr. Philippe Molaret from Thales Canada for their collaboration in this work.

## **References**

- [1] Sunil C. Patel, Manoranjan Majji, Bong Su Koh, John L. Junkins, Othon K. Rediniotis, *Morphing Wing: A Demonstration*

*of Aero Servo Elastic Distributed Sensing and Control*, Final research paper in 2005 Summer Research Experience for Undergraduates (REU) on Nanotechnology and Materials Systems, Texas Institute of Intelligent Bio-Nano Materials and Structures for Aerospace Vehicles (TiiMS) – NASA Research University, Texas A&M University, July 2005, College Station, Texas, USA.

- [2] [Shawn E. Gano, John E. Renaud, \*Optimized Unmanned Aerial Vehicle with Wing Morphing for Extended Range and Endurance\*, 9th AIAA/ISSMO Symposium and Exhibit on Multidisciplinary Analysis and Optimization, Atlanta, Georgia, USA, 4-6 September, 2002, pp. 1-9.](#)
- [3] David Cadogan, Tim Smith, Frank Uhelsky, Matt MacKusick, *Morphing Inflatable Wing Development for Compact Package Unmanned Aerial Vehicles*, 45th AIAA/ASME/ASCE/AHS/ASC Structures, Structural Dynamics and Materials Conference, Palm Springs, California, Apr. 19-22, 2004.
- [4] Popov, A.-V., Botez, R.M., Mamou, M., Mebarki, Y., Jahrhaus, B., Khalid, M., Grigorie, T.L., *Drag Reduction by Improving Laminar Flows Past Morphing Configurations*, AVT-168 NATO Symposium on the Morphing Vehicles, Evora, Portugal, 20-23 April, 2009.
- [5] [R.W. Wlezien G.C. Horner, A.R. McGowan, S.L. Padula, M.A. Scott, R.J. Silcox and J.O. Simpson, \*The Aircraft Morphing Program\*, AIAA-1998-1927.](#)
- [6] Thomas K. Bliss, Hilary Bart-Smith, *Morphing Structures Technology and its Application to Flight Control*, Student Research Conference, Virginia Space Grant Consortium - April 1, 2005, Newport News, Virginia, USA.
- [7] [Christopher E. Whitmer, Atul G. Kelkar, \*Robust Control of a Morphing Airfoil Structure\*, American Control Conference, June 8-10, 2005, Portland, Oregon, USA.](#)
- [8] [Pasi Ruotsalainen, Petter Kroneld, Kalervo Nevala, Timo Brander, Tomi Lindroos, Merja Sippola, \*Shape Control of a FRP Airfoil Structure Using SMA-Actuators and Optical Fiber Sensors\*. Journal of Solid State Phenomena, Volume 144 - Mechatronic Systems and Materials II, 2009, pp. 196-201.](#)
- [9] Amanda Lampton, Adam Nicksch, John Valasek, *Reinforcement Learning of a Morphing Airfoil-Policy and Discrete Learning Analysis*, AIAA Guidance, Navigation and Control Conference and Exhibit, 18 - 21 August 2008, Honolulu, Hawaii, USA.
- [10] Amanda Lampton, Adam Nicksch, John Valasek, *Morphing Airfoils with Four Morphing Parameters*, AIAA Guidance, Navigation and Control Conference and Exhibit, 18 - 21 August 2008, Honolulu, Hawaii, USA.
- [11] [Abdullah I. Al-Odienat, Ayman A. Al-Lawama, \*The Advantages of PID Fuzzy Controllers Over The Conventional Types\*, American Journal of Applied Sciences 5 \(6\): pp. 653-658, 2008](#)
- [12] Zdenko Kovacic, Stjepan Bogdan, *Fuzzy Controller Design – Theory and Applications*, Taylor and Francis Group, 2006

- [13] [Verbruggen, H. B. and Bruijn, P. M., "Fuzzy Control and Conventional Control: What is \(and can be\) the real contribution of Fuzzy Systems?" Fuzzy Sets Systems, Volume 90, Issue 2, September 1997, pp. 151–160.](#)
- [14] Rainer Hampel, Michael Wagenknecht, Nasredin Chaker, *Fuzzy Control – Theory and Practice*, Physica-Verlag, 2000
- [15] Zadeh, L. A., 1965. Fuzzy sets, *Information Control*, Vol. 8, pp: 339-353.
- [16] Jia Luo, Edward Lan, *Fuzzy Logic and Intelligent Systems - Fuzzy Logic Controllers for Aircraft Flight Control*, pp. 85-124, July 07, 2007, Springer
- [17] [Vick, A. Cohen, K., \*Longitudinal stability augmentation using a fuzzy logic based PID controller\*, Fuzzy Information Processing Society, 2009. NAFIPS 2009. Annual Meeting of the North American, pp.1-6, 14-17 June 2009](#)
- [18] Sefer Kurnaz ·Omer Cetin ·Okyay Kaynak, *Fuzzy Logic Based Approach to Design of Flight Control and Navigation Tasks for Autonomous Unmanned Aerial Vehicles*, *Journal of Intelligent and Robotic Systems* (2009) 54, pp. 229–244
- [19] [Ursu, I., Ursu, F., \*An intelligent ABS control based on fuzzy logic. Aircraft application\*, Proceedings of the International Conference on Theory and Applications of Mathematics and Informatics – ICTAMI 2003, Alba Iulia, pp. 355-368](#)
- [20] [Ursu, I., Ursu, F., \*Airplane ABS control synthesis using fuzzy logic\*, Journal of Intelligent & Fuzzy Systems: Applications in Engineering and Technology, Volume 16 , Issue 1, \(January 2005\), pp. 23-32](#)
- [21] [P Stewart, D Gladwin, M Parr, J Stewart, \*Multi-objective evolutionary–fuzzy augmented flight control for an F16 aircraft\*. Proceedings of the Institution of Mechanical Engineers, Part G: Journal of Aerospace Engineering, pp. 293-309](#)
- [22] [Altab Hossain, Aatur Rahman, Jakir Hossen, A.K.M. P. Iqbal, and SK. Hasan, \*Application of Fuzzy Logic Approach for an Aircraft Model with and without Winglet\*, International Journal of Mechanical, Industrial and Aerospace Engineering, 4:2, 2010, pp. 78-86](#)
- [23] [Hiliuta, A., Botez, R. M., and Brenner, M. \*Approximation of unsteady aerodynamic forces  \$Q\$ ,  \$k\$ ,  \$M\$  by use of fuzzy techniques\*. AIAA Journal, 2005, 43\(10\), 2093–2099.](#)
- [24] [Kouba, G., Botez, R. M., and Boely, N. \*Identification of F/A-18 model from flight tests using the fuzzy logic method\*. In Proceedings of the 47th AIAA Aerospace Sciences Meeting, Orlando, Florida, USA, 5–8 January 2009.](#)
- [25] [Boely, N., Botez, R. M., and Kouba,G. \*Identification of an F/A-18 nonlinear model between control and structural deflections\*. In Proceedings of the 47th AIAA Aerospace Sciences Meeting, Orlando, Florida, USA, 5–8 January 2009.](#)
- [26] [Grigorie, L.T., Botez, R.M., 2009, \*New adaptive controller method for SMA hysteresis modeling of a morphing wing\*, The Aeronautical Journal, Vol.114\(1151\), pp. 1-13.](#)
- [27] [Grigorie, L.T., Botez, R.M., 2009, \*Adaptive neuro-fuzzy inference system based controllers for Smart Material Actuator modeling\*, Journal of Aerospace Engineering, Vol. 223\(G6\), pp. 655-668.](#)
- [28] [Popov, A-V., Botez, R. M., Mamou, M., Grigorie, T.L., 2009, \*Optical sensor pressure measurements variations with\*](#)

*temperature in wind tunnel testing*, AIAA Journal of Aircraft, Vol. 46 (4), pp. 1314-1318.

- [29] Popov, A-V., Labib, M., Fays, J., Botez, R.M., 2008, *Closed loop control simulations on a morphing laminar airfoil using shape memory alloys actuators*, AIAA Journal of Aircraft, Vol. 45(5), pp. 1794-1803.
- [30] Sainmont, C., Paraschivoiu, I., Coutu, D., 2009, *Multidisciplinary Approach for the Optimization of a Laminar Airfoil Equipped with a Morphing Upper Surface*, NATO AVT-168 Symposium on "Morphing Vehicle", Evora, Portugal.
- [31] [Thomas Georges, Vladimir Brailovski, Emeric Morellon, Daniel Coutu, Patrick Terriault, \*Design of Shape Memory Alloy Actuators for Morphing Laminar Wing With Flexible Extradors\*, Journal of Mechanical Design, Vol. 31, No. 9, September 2009, 091006.](#)
- [32] [Brailovski, V., Terriault, P., Coutu, D., Georges, T., Morellon, E., Fischer, C., Berube, S., 2008, \*Morphing laminar wing with flexible extradors powered by shape memory alloy actuators\*, Proc. ASME Conf. Smart Materials, Adaptive Structures and Intelligent Systems \(SMASIS 2008\), Paper 337, Ellicott City, USA.](#)
- [33] [Coutu, D., Brailovski, V., Terriault, P., Fischer, C., \*Experimental validation of the 3D numerical model for an adaptive laminar wing with flexible extradors\*, 18<sup>th</sup> International Conference of Adaptive Structures and Technologies, Ottawa, Ontario, 3-5 October, 2007.](#)
- [34] [Coutu, D., Brailovski, V., Terriault, P., 2009, \*Promising benefits of an active-extradors morphing laminar wing\*, AIAA Journal of Aircraft, Vol. 46\(2\), pp. 730-731.](#)
- [35] [Terriault, P., Viens, F., Brailovski, V., \*Non-isothermal Finite Element Modeling of a Shape Memory Alloy Actuator Using ANSYS\*, Computational Materials Science, Vol. 36, No. 4, July 2006, pp. 397-410.](#)
- [36] [Tomescu B. \*On the use of fuzzy logic to control paralleled dc-dc converters\*. Dissertation Virginia Polytechnic Institute and State University Blacksburg, Virginia, October, 2001.](#)
- [37] Corcau, J. I., Stoenescu, E. *Fuzzy logic controller as a power system stabilizer*, International Journal of Circuits, Systems and Signal Processing, Issue 3, Volume 1, 2007, pp. 266-273.
- [38] J. Jantzen, *Tuning of fuzzy PID controllers*. Technical Report 98-H871, Department of Automation, Technical University of Denmark, September 1998.
- [39] [Kumar, V., Rana, K.P.S., Gupta, V., \*Real-Time Performance Evaluation of a Fuzzy PI + Fuzzy PD Controller for Liquid-Level Process\*, International Journal of Intelligent Control and Systems, Vol. 13, No. 2, June 2008, pp. 89-96.](#)
- [40] Mahfouf, M., Linkens, D. A., Kandiah, S., *Fuzzy Takagi-Sugeno Kang model predictive control for process engineering*, Printed and published by the IEE, Savoy place, London WCPR OBL. UK, 4 pp., 1999.